LASER INTERFEROMETER GRAVITATIONAL WAVE OBSERVATORY
- LIGO -
CALIFORNIA INSTITUTE OF TECHNOLOGY
MASSACHUSETTS INSTITUTE OF TECHNOLOGY

| **Technical Note** | **LIGO-T070044-00-Z** | 2007-02-13 |
|---|---|---|

# A Note on Calibration Issues at FSR

T. Fricke, S. Giampanis and A. C. Melissinos
*University of Rochester Stochastic Analysis Group*

*Distribution of this document:*

Stochastic Analysis Group

This is an internal working
note of the LIGO project

**California Institute of Technology**
**LIGO Project, MS 18-34**
**Pasadena, CA 91125**
Phone (626) 395-2129
Fax (626) 304-9834
E-mail: info@ligo.caltech.edu

**Massachusetts Institute of Technology**
**LIGO Project, Room NW17-161**
**Cambridge, MA 02139**
Phone (617) 253-4824
Fax (617) 253-7014
E-mail: info@ligo.mit.edu

WWW: http://www.ligo.caltech.edu/

# 1 The calibration procedure for the LIGO interferometers

Since we can not inject a gravitational wave (of known frequency and amplitude) we calibrate the interferometer by changing the length of the arm cavities. This is achieved by moving the end test mass of the two arms in a differential manner. A (sinusoidal) current is driven through the control coils and these impart an oscillatory force to the test mass, along the cavity axis, at the drive frequency. The test masses are suspended and react to this force as a pendulum. To first approximation the natural frequency of the pendulum is $f_0 = 0.74$ Hz.

The change in the cavity length induces a phase shift on the carrier returning to the anti-symmetric port (AS) and thus simulates the effect of a gravitational wave. We directly relate a displacement $\Delta x$ of the end mirror to an (optimally oriented) gravitational wave of strain $h = \Delta x/L$. We are interested in the interferometer response as a function of the frequency $f$ of a (monochromatic) gravitational wave. Yet calibration is done only at three distinct frequencies. The response at all frequencies is obtained from two models which use the three calibration values as inputs. Only one input would suffice to "normalize" the models but the agreement at the other two frequencies provide an important consistency check of the *interferometer model* and of the *test mass motion model*.

The *test mass motion model* gives the amplitude of the test mass oscillation as a function of excitation current. The model itself must be calibrated empirically. This is done at DC where the test mass is driven slowly and fringes are counted at the dark port. To extrapolate to the frequencies of interest we treat the test mass as a simple pendulum well above resonance ($f_0 = 0.74$ Hz)

$$\begin{aligned} x(f) &= x_{DC} \left\{ \left[1 - (f/f_0)^2\right]^2 + \left[(1/Q)^2 (f/f_0)^2\right] \right\}^{-\frac{1}{2}} \\ &\simeq x_{DC} (f_0/f)^2 \end{aligned} \tag{1}$$

The DC value $x_{DC}$ can be determined quite precisely as a function of the excitation current. Equation (1) gives $x(f)$ to good accuracy for $f \leq 1$ kHz, but the extrapolation becomes less certain at higher frequencies. This is so because the correction factor $(f_0/f)^2$ is of order $10^{-6}$ implying a force $10^6$ larger than at DC to drive the test mass at the same amplitude. This in turn introduces nonlinearities in the driving circuits and leads to excitation of the internal modes of the test mass. Even the validity of Eq. (1) may be questioned.

To circumvent in part the need for an empirical calibration of the applied force, recently a laser beam has been used to drive the test masses (through its radiation pressure which can be calculated from the laser power). The laser can be modulated to arbitrarily high frequencies without loss of linearity. Results from this effort show good agreement with the standard calibration method at low frequencies but discrepancies at the 20% level for $f \sim 1$ kHz. Unfortunately there is not enough power in the laser to impart detectable oscillation

amplitude to the test mass at ∼37 kHz.

The *interferometer model* has two components. The first is to calculate the optical gain in the arm cavities as a function of frequency. This is quite straightforward since the behavior of an optical (Fabry-Perot) cavity is uniquely determined by the reflectivity of its mirrors. The latter are determined in situ by measuring the $Q$ of the cavity through the storage time of the light; what is referred to as the "cavity pole" measurement.

The second component involves the calculation of the effects of the electronic feedback on the signal detected at the antisymmetric port. This takes the form

$$ASQ(= \text{ signal}) = x_{in}\frac{C(f)}{1+G(f)} \tag{2}$$

and is a strong function of frequency. In Eq. (2), $C(f)$ is the optical gain in the cavity and $G(f)$ is the *open loop gain* (including the actuation function); $x_{in}$ has been determined from the test mass motion model. $C(f)$ can be calculated (up to normalization) from the interferometer model mentioned above. $G(f)$ is calculated from the parameters of the filters in the feedback loop and is checked against measurements made at the beginning of (and occasionally throughout) the run.

# 2 Calibration at the fsr frequency

The effects of mirror motion at 37 kHz have been investigated by two different groups in the past and are discussed in the following section. Such measurements however are too invasive to be considered during (or in the preparation stages of) a run. Furthermore they suffer from the serious limitations already discussed.

Instead, the *fast channels* (sampled at 262,144 Hz) were calibrated at two of the standard low frequency calibration lines (∼400 and 1100 Hz). Indeed this leads to an *exact* calibration at the fsr frequency. This is because of two reasons: (a) The open loop gain at the fsr is null, $G(f) = 0$, since no feedback is effective at this frequency. (b) The optical gain in the cavity at the fsr equals the optical gain at DC. Thus Eq. (2) simplifies to

$$ASQ\,(f_{fsr}) = x_{in}g_W(f)C(f=0) \tag{3}$$

where $g_W(f)$ is the gain of a whitening filter in the fast channel. A schematic comparison of the low frequency and fast channel DAQ paths is shown in Fig.1

The whitening filter gain has been measured (in fact it cuts off the lowest of the calibration lines, $f \sim 40$ Hz, which therefore is not observable in the fast channel). $C(f = 0)$ is ob-

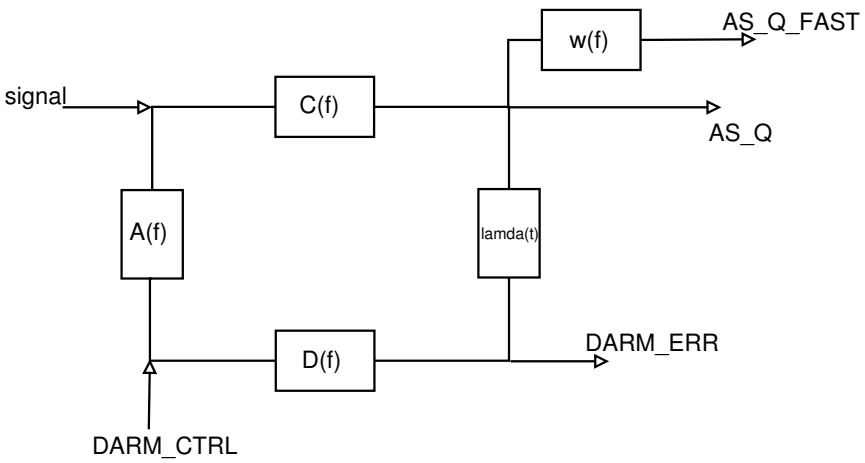


Figure 1: Block diagram of DARMloop model

tained from the calibration lines (consistently from both lines). Finally the (rapid) frequency dependence around the fsr is obtained from the F-P cavity model using the "cavity pole" measurement.

Our model and procedures are validated by comparing the calibration constants extracted from the fast channels to those obtained by the calibration group [1] (see *Calibration of Fast Channels*). We emphasize that we are *extrapolating to DC* (which is equivalent to extrapolating to the fsr) *just as is done in the standard procedure* for the calibration of the low frequency region. The absence of open loop gain at the fsr, further improves the robustness of the determination of the calibration.

The calibration was done using the fast channels while the data that is analyzed for the physics results is obtained from the heterodyned 1 fsr and 2 fsr channels. Thus we must check that the heterodyned data has not been corrupted. We do this by comparing the amplitude of the lines originating from the thermal excitation of the test mass resonances in the fast and heterodyned channels. The spectrum around the 1 fsr (before applying the calibration) is shown in Fig.2

These features are very distinct and repeatable and have been tracked from the S3 through the S5 runs. They are well understood, and under high resolution reveal the fine structure arising from the different test masses contributing to the spectrum.

We compare the amplitude of these lines in the fast and heterodyned channels (under the same bandwidth) and find good agreement [1]. Finally the rich and reproducible spectrum that is observed in the heterodyned (i.e. data) channels assures that the DAQ is working properly in the high frequency region.

The final issue has to do with the time dependence of the calibration. For the standard channels this is done by continuously tracking the calibration lines and providing a list of correction coefficients $\alpha(t)$ and $\beta(t)$. For the S4 data the fast channel calibration was done only before the run and the coefficients $\alpha(t)$ were used to correct the calibration during the

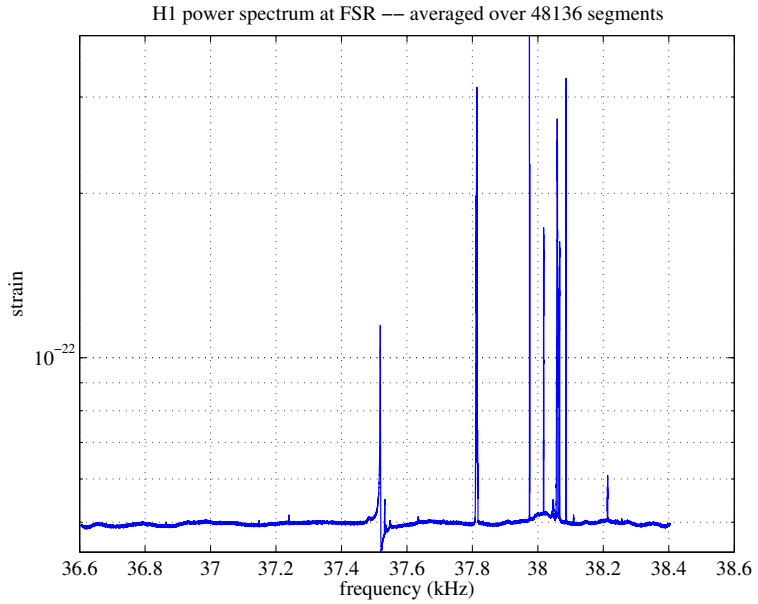


Figure 2: H1 spectrum during S4

runs. This is described in [2] (see *S4 paper*). To track possible calibration changes of the fast channels during the S4 run we rely on the thermal excitation lines as discussed in section 4. Note that this problem does not exist for the S5 run where the fast channel calibration was continuously monitored through the 0fsr (heterodyned) channel available in the Level 1, RDS frames.

# 3 3. Direct measurements of excitation at the fsr frequency

Measurements of the interferometer response to cavity length changes were carried out in 2002 and 2003 by R. Savage, M. Rachmanov and collaborators [3] (see *Characterization of LIGO 4-km Fabry-Perot cavities via high-frequency dynamic responses to length and frequency variations*) and by W. Butler and A. Melissinos [4] (see *Characterization of the High Frequency Response of LASER Interferometer Gravitational Wave Detectors*). Such measurements completely confirmed the model for the optical gain of the cavity. This is the model that is being used for establishing the calibration (both at the fsr and at low frequencies) as discussed in the previous section. We will refer to the results from these investigations in order to show that the interferometer has been extensively characterized in the fsr region and that it's response is well understood. This fact is sometimes overlooked in discussions about the fsr data.

We will follow ref. [4] even though similar data and conclusions were obtained in ref. [3]. We start with Figs. 3.18 through 3.22 of [4] which demonstrate that the signal at the AS port, generated by test mass motion is perfectly fitted by the interferometer model (up to

an arbitrary normalization). These fits include subtle features arising from the presence of the recycling cavity.

Figure 4.1 shows that the effects of the excitation of the internal modes of the test mass can also be properly modeled. The data in Figs. 3.18-3.22 and Fig. 4.1 were taken in a "swept sine" mode. The response to fixed frequency excitation is shown in Figs. 4.2-4.4. In this case the BW resolution can be narrowed to reveal the sidebands from the *up converted* low frequency modes of oscillation. Such modes couple nonlinearly to the "acoustic" mode which is driven by a distorted sinusoid (due to the very strong drive current).

Figures 4.6 and 4.7 give typical shapes of the test mass excitation at low and high frequency (compliments of D. Coyne). Clearly, the high frequency mode has very poor overlap with the shape of the carrier (laser) beam. Thus one *can not* expect to obtain the correct normalization factor from an *active displacement* procedure at the fsr.

A discussion of the calibration at the fsr for the S5 run can be found in [5] (see *Fast Channel Calibration for S5*).

# 4 Time dependence of the S4 calibration

As we know, for the S4 run the direct calibration of the fast channels was done only before the run. At this point we also established that the heterodyned channels were faithful copies of the fast channel in the appropriate frequency bands.

Since we had no calibration lines during the run we used the thermal excitations as surrogates. These lines are narrow, at fixed frequencies and (if averaged for a time much longer than their natural relaxation period) of fixed amplitude. Of course their phase is arbitrary.

The power in the thermal line (acoustic peak) at $= 37,813$ Hz (for H1) was measured for every frame of the S4 run and then averaged over $10^4$ s intervals. Fig.3 shows the histogram of the distribution of the averaged power. It has a dispersion $\sigma/\text{mean} = 0.11$. Since the calibration is given in terms of spectral amplitude, the dispersion of the fsr calibration during the S4 run is $\sim$6%. This is less than our estimated calibration uncertainty and has been folded in the final uncertainty [2].

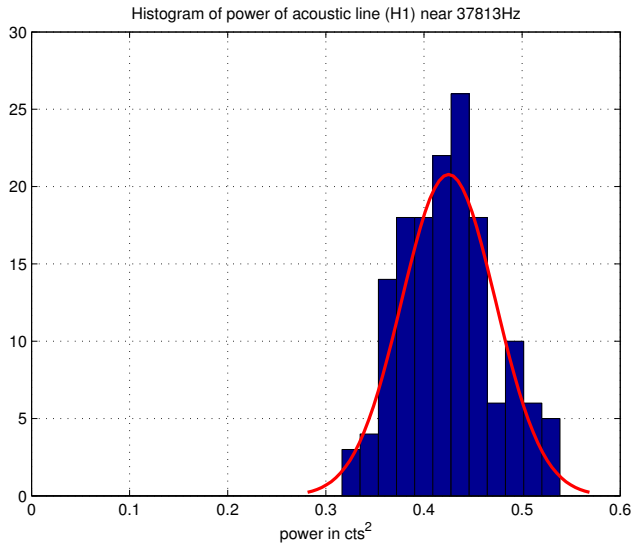


Figure 3: Histogram of power of acoustic line in H1